Wireless Power Transfer, 2018, 5(2), 87–96.
doi:10.1017/wpt.2018.1

RESEARCH ARTICLE

Low-cost wireless power efficiency optimization of the NFC tag through switchable receiver antenna

YI ZHAO[1], HUAYE LI[1,2], SAMAN NADERIPARIZI[1], AARON PARKS[1] AND JOSHUA R. SMITH[1,2]

Near-field communication (NFC) readers, ubiquitously embedded in smartphones and other infrastructures can wirelessly deliver mW-level power to NFC tags. Our previous work NFC-wireless identification and sensing platform (WISP) proves that the generated NFC signal from an NFC enabled phone can power a tag (NFC-WISP) with display and sensing capabilities in addition to identification. However, accurately aligning and placing the NFC tag's antenna to ensure the high power delivery efficiency and communication performance is very challenging for the users. In addition, the performance of the NFC tag is not only range and alignment sensitive but also is a function of its run-time load impedance. This makes the execution of power-hungry tasks on an NFC tag (like the NFC-WISP) very challenging. Therefore, we explore a low-cost tag antenna design to achieve higher power delivered to the load (PDL) by utilizing two different antenna configurations (2-coil/3-coil). The two types of antenna configurations can be used to dynamically adapt to the requirements of varied range, alignment and load impedance in real-time, therefore, we achieve continuous high PDL and reliable communication. With the proposed method, we can, for example, turn a semi-passive NFC-WISP into a passive display tag in which an embedded 2.7″ E-ink screen can be updated robustly by a tapped NFC reader (e.g. an NFC-enable cell-phone) over a 3 seconds and within 1.5cm range.

Keywords: NFC, Wireless Power, Display, Antenna optimization

Received 3 December 2017; Accepted 11 February 2018; first published online 25 April 2018

I. INTRODUCTION

Near-field communication (NFC)-enabled smart-phones or other NFC readers used in buses, stores, and buildings make NFC technology ubiquitous to almost everywhere. Leveraging on-tag logic, larger memory, and more secure protocol, NFC has become a promising technology to replace Bar-code. Because of the low cost (a few cents), battery-free, and tap-to-go features, the NFC tag/card is widely used nowadays for access control, credit card payment, and logistic management [1, 2].

Generally, the power consumed by single NFC tag in those applications comes from the magnetic signal transmitted by an NFC reader. Other than providing tiny data transfer for identification purposes, NFC can become a cost-efficient charging interface for portable devices. Commercially available NFC readers can transmit up to 750 mW continuous wireless power [3] which can be used to energize some low-power smart devices. As an example, Battery-free passive NFC tag with enhanced computation and sensing features can be powered from commercially available NFC readers. These battery-free tags have many applications in healthcare management, patient monitoring [4–6], and intelligent retail. Our previous work presents a software-defined NFC tag called NFC wireless identification and sensing platform (WISP) [1, 7, 8]. Using a single high-Quality factor (Q) receiver antenna and a multi-stage rectifier to implement an efficient power harvester, the NFC-WISP hardware has a higher power harvesting efficiency comparing to existing NFC tags when tapped to an NFC reader. Besides, this platform leverages a general-purpose micro-controller, therefore, it is easily programmable for distinct applications with different on-board peripherals (such as temperature sensors, inertial measurement unit (IMU) sensors, nonvolatile FRAM memory, E-ink display, battery, etc). NFC-WISP can also be extended to more complex/custom applications through the extension headers and using a custom designed expansion shield. For example, the NFC-WISP can be used as a battery-free NFC temperature sensor by enabling the on-board thermometer, or it can be used as a semi-passive bi-stable E-ink display tag with the assistant of a re-chargeable battery.

[1]Department of Electrical Engineering, University of Washington, Seattle, USA
[2]Department of Computer Science & Engineering, University of Washington, Seattle, USA
Corresponding author:
Joshua Smith
Email: jrs@cs.washington.edu.

An earlier version of this article was published with an incorrect expansion of the acronym WISP. This has now been corrected.

A) Challenge

The amount of power received by an NFC tag from a reader is limited by its antenna specs and alignment, load impedance, range, and the transmit power, most of which fluctuate in different use cases. Besides, performing power demanding tasks (more than 1 mW) on the NFC tags or NFC-WISP is very challenging. For instance, updating an E-ink display on the NFC-WISP tag usually takes much more power ($\approx$ 30 mW) than the continuously harvested power (max 6 mW if using a cell-phone reader [1]). To overcome this challenge, the previous NFC-WISP design utilizes a small re-chargeable battery to buffer enough energy required for updating an E-ink. NFC-WISP then duty-cycles the display update operation at a rate such that the average consumed power by NFC-WISP is less or equal to average harvested power. But the use of battery limits the NFC-WISP's life-time and increases the maintenance overhead, size, and cost of the hardware.

Another challenge that commercially available NFC tags or NFC-WISPs [1] suffer from is the limited placement freedom of the tag which constrains the usability of the NFC technology in practice (such as limited range and perfect antenna alignment requirements). For example, the antenna misalignment and changing in the tag's position and orientation, which may be varied with different users and use cases, can easily result in the failure of NFC communication. In addition, in our NFC-WISP applications, such as temperature logging and display, the different run-time processes or the use of distinct peripherals may result in the different load impedance of the NFC tag, thereby changing the power delivered to the load (PDL) or NFC communication performance. Disconnecting the load while delivering wireless power or doing communication can solve the problem of load variance, but it dramatically delays the application processing speed, which is already slow in passive tag scenarios.

Optimizing both PDL and communication performance is challenging because of a fundamental trade-off between wireless power efficiency and bandwidth of magnetic coils coupling. While a high coupling bandwidth is critical for ensuring robust and high-performance NFC communication, wireless power delivery efficiency boosts at lower coupling bandwidth. Traditionally, a single multi-turn loop coil is used in both NFC transmitter (reader or phone) and receiver (tag) to establish magnetic coupling for power delivery as well as in-band communication. Typically, high PDL achieved by using high-quality factor (Q) antenna, results in a narrow resonating bandwidth, therefore, limits the tag's reading distance and freedom of antenna alignment. The available space for increasing the Q of the transmitter (Tx) antenna in commercially available NFC readers is very limited and the modification cost is too expensive, especially in an NFC-enabled smart phone. For example, the intrinsic Q of the NFC antenna in the Nexus phone is around 15 [9]. Generally, the NFC ISO 14443 Type B protocol can maximize the transmitted power and communication speed due to the use of 10% amplitude-shift keying in its down-link as well as high communication bandwidth, which is critical for enabling power-hungry applications with large communication payload, such as updating display image on a display tag [1, 7]. Other protocol, such as ISO 14443 Type A and ISO 15693, either has limited transmitted power due to 100% modulation depth or slow communication speed [10, 11]. However, the ISO 14443 Type B tag requires a very low Q resonating system to provide a high bandwidth of minimal 1.906 MHz MHz to ensure successful up-link communication. This means, although the use of a high Q resonating design results in higher power delivery, it makes the communication of the NFC tag extremely vulnerable to the change of position, and is likely to result in the failure of data transfer. In practice, different users' usage habits and scenarios, which can cause significant range and antenna alignment variation, severely limit the performance of the system.

B) Prior work

Traditional near-field wireless power delivery systems [12–15], which are very similar to the NFC system but without communication features, use different numbers of coils (generally 2–4 coils in total) for different power transfer requirements. In a nutshell, the more coils used, the more parameter knobs are available for system optimization in terms of obtaining the highest power delivered to the load, optimal power delivery range and tolerance to the load variation. Our analysis [2] shows that, if considering all the parasitic effects in practice, a 3-coil NFC system (with one high Q loop and one low Q load connected coil on the receiver and one coil on the transmitter) can deliver more power at smaller k while having limited communication performance (k is the magnetic coupling coefficient and negatively co-relative to the Transmitter(Tx)-to-Receiver(Rx) distance). On the other hand, a 2-coil system (single low Q receiver coil and one coil on the transmitter) has a wider resonant bandwidth and a better communication performance when k is very high but obviously lower power delivery efficiency.

C) Proposed idea

To overcome the above challenges, in this paper, we present a method, which can switch the NFC system between 2-coil and 3-coil configuration (including both Tx and Rx coils) to improve the wireless power delivery efficiency and obtain a reliable NFC communication. A programmable multi-coil receiver antenna controlled by a radio frequency switch is used for a new NFC-WISP 2.0 hardware. In addition, we show the challenges and trade-offs in the NFC wireless power delivery system, especially, when using an NFC-enabled phone as the power source. By finding the design sweet-spots, we ensure high power delivery as well as high bandwidth communication in different operation states or scenarios. Our contributions are listed and summarized below:

1. A theoretical analysis of the PDL given two distinct receiver antenna configurations in the NFC system is discussed.
2. A simulation work considering the variation of receiver load and fluctuation of reading distance or antenna alignment is presented.
3. The proposed method is implemented in a new version of the NFC-WISP 2.0, in which a configurable multi-coil receiver antenna is designed and discussed. It is illustrated how the 2-coil/3-coil switching method improves the system PDL, range, and communication robustness given varied system loads and states. The designed antenna is flexible so it can fit any curved surface and enable more applications.
4. The improved NFC-WISP hardware is shown to be used for battery-free but power-hungry applications with maximum operation duty-cycle and a cell-phone reader.

As far as the author's knowledge, it is the first high-performance battery-free NFC tag that can be used to robustly update a 2.7″ E-ink display over the time period of 3 seconds and within upto 1.5 cm reading range in all usages and scenarios.

5. A smart label application using the designed NFC-WISP display tag and a customized Android application (App) in a smart-phone is demonstrated. The App allows the user to choose and edit an RGB photo from the phone, process it into a clear black and white sketch picture, and update the display of the NFC-WISP by tapping the phone onto the tag for only 3 seconds with a large 1.5 cm alignment tolerance.

II. OPTIMIZATION APPROACHES FOR THE NFC WIRELESS POWER SYSTEM

A) Optimization challenges and solutions

NFC reader can operate in three modes for different applications. When an NFC reader is in tag reader/writer mode, it can transmit about tens to hundreds of milliwatts of wireless signal into the air [1, 3]. We design a passive/battery-free tag, NFC-WISP 2.0, to harvest the transmitted power from a magnetic coupled NFC reader. The obtained power is not only used for traditional NFC communication but also for any other enhanced features, such as computation, sensing, and display. The newly developed NFC-WISP tag is shown in Fig. 1, an NFC-enabled Galaxy Nexus phone is used as the reader for demonstration purpose in this paper. The previous NFC-WISP 1.0 hardware [1] uses either a battery or a supper-capacitor to store harvested energy; whereas the new NFC-WISP 2.0 tag only utilizes a 500 μF ceramic capacitor to buffer the harvested energy. In general, to enable more power-hungry applications other than NFC communication running on the NFC tag, not only the NFC reader has to keep sending data (useful or dummy) in order to deliver sufficient power to the NFC-WISP tag, but also the NFC-WISP PDL performance has to be continuously high enough in all practical scenarios to prevent the system from brownouts. Demanding applications, whose power requirements exceed the instantaneous power harvested from the NFC reader, require duty-cycling and a large energy buffer (such as a super-capacitor or a battery) to store sufficient energy that can energize at least one operation cycle for a certain process. However, the use of the super-capacitors or batteries has many limitations: super-capacitors have higher leakage comparing to small ceramic capacitors and, therefore, limit the energy harvesting performance of the NFC-WISP; Besides, super-capacitors can provide smaller source current which avoids enabling applications with higher power consumption requirement; Batteries, especially Lithium-based batteries, have limited lifetime and its performance degrades over time. In addition, batteries and super-capacitors generally have a larger size and are more expensive comparing to a small ceramic capacitor, which is critical for space limited wearable or Internet-of-Things (IoT) applications [16]. Increasing the PDL of the NFC-WISP system is a proper approach to solve the challenges caused by the use of a battery or a super-capacitor, besides, higher effective harvested power can further improve the operation speed, or in the other words, increase the duty-cycle. This plays a key role to achieve better usability and user experience. In the application section, we demonstrate how the new passive NFC-WISP 2.0 tag with improved PDL is able to update a display two times faster than what can be achieved by the battery-assisted NFC-WISP 1.0 hardware [1].

Increasing the Quality Factor (Q) of the NFC reader (Tx) or the tag (Rx) antenna seems to be a method to improve PDL. However, the increase of the Q may not necessarily result in the maximum PDL given all reading ranges or receiver load impedance variations. In addition, high Q system design will limit the bandwidth of the system and dramatically degrade the NFC communication performance. When the NFC phone exchanges target data with the tag, especially during up-link (tag-to-reader communication), a high bandwidth of about 1.906 MHz is required because of the use of ISO 14443 protocol [17]. Due to the fundamental trade-off between bandwidth and Q, the NFC-WISP 2.0 tag has to adapt to the different requirement of Q and bandwidth in the different run-time period even in the same application. The system requires higher bandwidth during NFC communication process, thereby resulting in the lower system Q. In this particular case, the high bandwidth should be given the highest priority rather than wireless power performance; after the communication period, especially the up-link, has ended, the NFC reader or cell-phone can be configured to stream dummy data to power the tag. At this moment, NFC-WISP should maximize the Q to increase PDL efficiency.

As mentioned earlier, load impedance variations of the NFC-WISP during run-time is another parameter that can negatively impact the performance of NFC-WISP as well. Adaptive frequency or impedance tuning method is implemented in some of the wireless power transmitters [12, 15, 18–20] to compensate for the load variations of the NFC tags during run-time. However, the implementations of

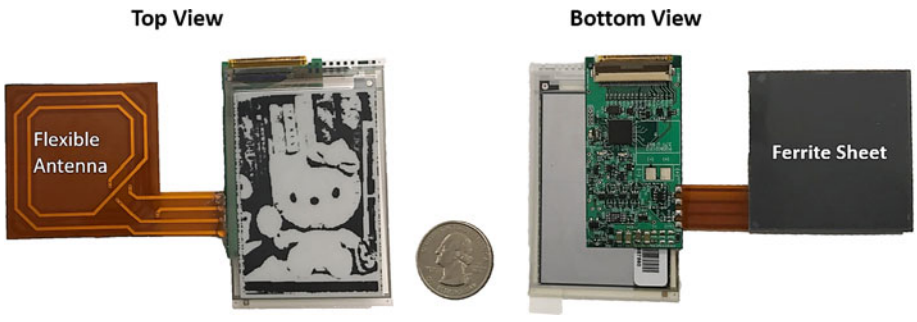

Fig. 1. Prototype of new battery-free NFC-WISP with flexible switchable receiver antenna and 2.7″ E-ink display.

frequency or impedance tuning on commercially available NFC readers is challenging due to the following reasons; (a) the change of receiver load can occur within a short period (a few ms), the large controlling delay of the adaptive tuning methods makes the millisecond-level tuning very challenging or expensive. (b) frequency tuning violates both the NFC protocol and FCC regulations.

Therefore, we present a low-cost receiver antenna design in the new NFC-WISP 2.0 hardware to adapt to different system requirements at run-time and maintain high performance in different conditions. The receiver antenna of the NFC-WSIP 2.0 consists of two coils (Figs 1–3), one is high Q and is configured as a single frequency resonator with a tuning capacitor; the other is low Q and is connected to the receiver load. We use a switch controlled by the on-board microcontroller to control the wireless coupling between the high-Q resonator and the rest of the system. When the switch is off, the high Q resonator is open circuits and the NFC-WISP becomes a low Q receiver system; when the switch is on, the high Q coil gets attached and magnetically couples with the existing low Q receiver coil on the tag to create a totally different system in terms of Q and bandwidth. The detail system optimization analysis and approach are discussed in the following sections.

B) Circuit model and system analysis

The circuit model of a 2 or 3-coil NFC wireless power system is presented in Figs 2 and 3. We simulate the system with three different *Rx* configurations given the same *Tx* and system load (V_s, R_s, C_1, R_{p1}, L_1, R_{load} remain constant): one is a 3-coil system and the other two are 2-coil systems. The overall Q of the wireless coupling link is dominated by the highest Q coil in the *Rx*. In a 3-coil system, the highest-Q *Rx* coil is L_2 and the 3rd coil connected to the load has a lower Q. The coupling coefficient k_{12} in the 3-coil system and k_{13} in the 2-coil system refer to the NFC reading distance and antenna alignment. In theory, the smaller the reading distance and the stronger the *Tx*-to-*Rx* coupling, the higher the k value. In the 3-coil system, k_{23} is optimized for maximizing the average PDL over a 3 cm *Tx*-to-*Rx* range.

When using a smart-phone as an NFC reader, which comes with small *Tx* antenna dimensions and provides a low transmitting power, there are some limitations and assumptions as follows:

1. the max coupling coefficient k between the smart-phone reader and the NFC-WISP is estimated as 0.42 based on the dimension of the *Tx* antenna of a Nexus phone and NFC-WISP tag's antenna (which is 45 mm × 45 mm, 4 turns loop coil).
2. the ISO-14443 Type B NFC protocol requires at least a resonant bandwidth of above 1.906 MHz [17] due to its specific communication requirements, which is 5–20 times higher than typical wireless power systems [12, 19, 21, 22].
3. In practice, the NFC tag reading range varies with humans" usage. Therefore, the design of the system should have a large tolerance to the change of relative antennas" position. In another word, the PDL and the NFC-WISP resonating bandwidth should be optimized given a large variation of k (overall system coupling coefficient variation due to antennas" misalignment).
4. Due to the load impedance variation of the NFC-WISP with peripherals and run-time software operating states, the design of the inductively coupled wireless power NFC system should be less sensitive to the change of load impedance. That means the optimization goal is to jointly optimize the PDL efficiency and the communication performance given the load variation as well.

From our previous paper [2], we find that parasitic capacitance between each coil and the coupling between non-adjacent coils (L_1-to-L_3) result in significant resonant frequency shifting and PDL variation as k increases (the coupling becomes stronger). This prevents us from obtaining high-quality wireless power and communication performance in an NFC wireless power system. In general, the low Q_2-coil system can achieve an optimized PDL at larger k and the high Q_3-coil system can achieve an optimized PDL at smaller k. Briefly, given the same receiver load impedance, the 2-coil system can achieve better power transfer at a very close *Tx*-to-*Rx* range; In comparison, the 3-coil can lead to higher PDL at a larger range. However, the optimized PDL and its best range differ between 2-coil and 3-coil system and vary as the load impedance changes. In the following section, we explain how we can achieve PDL optimization with different k and receiver load impedances using our proposed switchable receiver antenna architecture design.

C) Load impedance variation

We simplify the reflected impedance from the load to the transmitter antenna in both 2-coil and 3-coil systems in equation (1). k_{13} is ignored here to simplify the theoretical analysis. We will include the effect of k_{13} and other parasitic effects discussed in [2] in the following section. The Q_{2L_3} refers to the loaded Q of the entire two coils of the receiver in a 3-coil system, the Q_{3L_2} refers to the loaded Q of the single receiver coil in a 2-coil system. In general, the Q_{2L_3} is designed larger than Q_{3L_2}. Only when the RL is much smaller than the antenna parasitic resistance R_{p1}, the Q_{2L_3} will become larger than Q_{3L_2}. In most of the cases, by adding additional receiver coil, the reflected impedance seen by the transmitter becomes higher given the same receiver load impedance R_L of the 2-coil system. That explains why, in the previous simulation, the 3-coil system has better wireless power efficiency in the far range (small k) while the 2-coil system has better performance in close range (large k). The maximized power delivery efficiency happens when the reflected load impedance conjugate

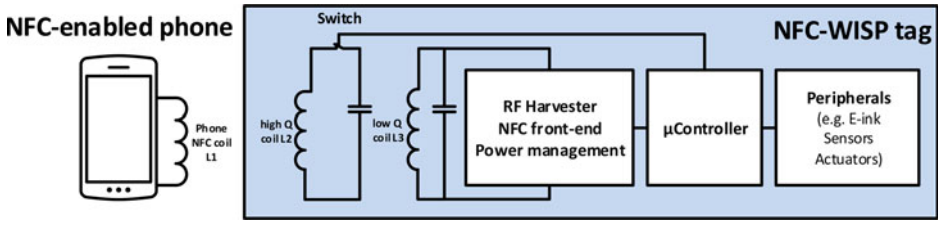

Fig. 2. Architecture of passive NFC-WISP 2.0.

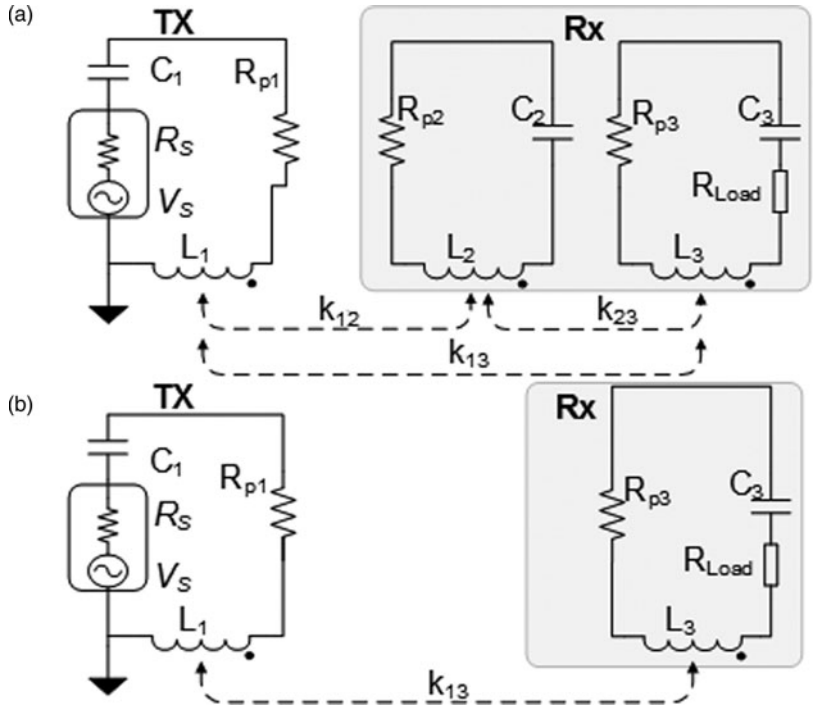

Fig. 3. Block diagram of the NFC wireless power system: (a),(b) refer to 3-coil and 2-coil systems respectively. *Tx* is the NFC reader and *Rx* is the NFC tag. R_{pi} and C_i are the equivalent resistance and tuning capacitance of the coil i with inductance of L_i. R_s and R_{load} are the source resistance of NFC reader and the equivalent resistance of the loaded hardware on the NFC tag. k_{ij} is the coupling coefficient between coil i and coil j.

matches the source impedance of the transmitter; as the range becomes closer, the reflected impedance becomes larger because of the stronger magnetic coupling. We call the coupling coefficient and the *Tx*-to-*Rx* distance where the n-coils system can match the transmitter source impedance as k_{mn}, d_{mn}. Since the reflected load impedance is an increasing function of k (k_{13} in the 2-coil system, k_{12} in 3-coil), the 3-coil system is likely to match the same source impedance at smaller k (longer distance). However, when the receiver load R_L is too small (similar or smaller than R_{p1}), Q_L becomes extremely large and dominates the Q_{L3}, therefore resulting in larger reflected impedance in a 2-coil system rather than a 3-coil system at smaller k. However, in this case, the best impedance matching happens at a very smaller k_{mn} (normally large d_{mn}), where, the absolute PDL becomes much smaller due to the long signal propagation distance. Compared to the case where the R_L is medium and large, the PDL is much smaller when R_L is too small over the same NFC reading range (03 cm). A medium R_L can achieve impedance matching at larger k_{mn} or smaller d_{mn}, thus resulting in large PDL.

$$
\begin{aligned}
R_{ref21_3} &= k_{12}^2 Q_1 Z_1 \times \frac{Q_{2_3}}{1 + k_{23}^2 Q_{2_3} Q_{3L_3}} \quad (3-\text{coil}) \\
&= k_{12}^2 Q_1 Z_1 \times Q_{2L_3} \\
Q_{2L_3} &= \frac{Q_{2_3}}{1 + k_{23}^2 Q_{2_3} Q_{3L_3}} \\
Q_{3L_3} &= \frac{Q_{3_3} Q_L}{Q_{3_3} + Q_L} \\
R_{ref31_2} &= k_{13}^2 Q_1 Z_1 \times Q_{3L_2} \quad (2-\text{coil}) \\
Q_{3L_2} &= \frac{Q_{3_2} Q_L}{Q_{3_2} + Q_L}.
\end{aligned}
\tag{1}
$$

In the most wireless power systems, the receiver antenna is designed not only to optimize the impedance matching to the transmitter but also to match the load impedance, which determines the optimal distance d_{opt} where PDL is maximized. In a 2-coil system, there might be some impedance values for the transmitter and the receiver that cannot be matched given a particular load R_L within the range d [13]. In a 3-coil system, because of the use of one additional coil, we have more knobs to turn (k_{23}, Q_2) to optimize the impedance matching given any load R_L within the same range d. The desired NFC reading range in most applications is 3 cm. Therefore, in this new revision of NFC-WISP design, we use an empirical k_{23}, which is optimized for obtaining better impedance matching over the target NFC-WISP reading range.

In practice, the load impedance R_L may change between different processes in real-time. For example, in the cold start state, the NFC-WISP begins from zero power to power-on mode after harvesting enough energy. The load impedance R_L of the NFC-WISP in this state is represented as $R_{L_{coldStart}}$ (around 1 ohm in our measurement). However, after the NFC-WISP has been charged up and enters sleep mode, waiting for NFC reader interaction, the load impedance R_L of the NFC-WISP becomes $R_{L_{sleep}}$, which is larger than $R_{L_{coldStart}}$ in our measurement. When the NFC-WISP is running power-hungry tasks, such as updating E-ink display (E-ink updating mode) or transmitting data to the NFC-enabled phone (*Tx* mode), it draws a significant amount of current (typically around 1–5mA) from the onboard energy storage element, the R_L of the NFC-WISP then becomes $R_{L_{E-ink}}$ and $R_{L_{Tx}}$, which are larger than $R_{L_{sleep}}$. The variance of the load impedance is mainly introduced by the change of parasitics in the rectifier circuits and the changes of current drawn by the rest of the systems. (Please note that all the load impedance R_L mentioned above is

Table 1. Smart-phone and NFC-WISP measurements..

R	Ω	R	Ω	L	μH	Coil Q		Q_{3L}	
$R_{L_{coldStart}}$	1	R_{p1}	7.7	L_1	1.48	Q_1	16.4	Cold start	13.5
$R_{L_{sleep}}$	18	R_{p2}	6	L_2	1.56	Q_2	22.2	Sleep	1.9
$R_{L_{Tx}}$	34	R_{p3}	1.77	L_3	0.44	Q_3	21	tx	1
$R_{L_{E-ink}}$	43	R_s	18					E-ink	0.8

equivalent serial impedance measured from Vector Network Analyzer given 13.56 MHz transmitted frequency and the imaginary impedance is matched with tuning capacitor).

Therefore, the problem becomes: given a particular R_L, how to choose the receiver antenna configuration (single receive coil or two) to optimize power delivery efficiency as well as keeping communication performance within the targeted NFC-WISP-to-Reader range (around 3 cm). Therefore, the designed antenna of NFC-WISP 2.0 can be switched to a low Q receive mode with a single receive coil (2-coil system) by opening the middle coilL_2, and can be switched to high Q receiver mode with two receive coils (3-coil system) by closing the middle coil loop L_2 (see Fig. 3). The architecture and prototype of the new NFC-WISP are shown in Figs 1 and 2. The measured parameters of the smart-phone reader and NFC-WISP are presented in Table 1.

Considering all the parasitic effects mentioned in the previous chapter, the simulated PDL when the NFC-WISP is in different states is illustrated in Fig. 4. From the simulation results, we can find that when $R_L = R_{L_{coldStart}}$, the PDL value becomes very small, because we use a parallel-connected tuning capacitor for tuning the NFC-WISP, which results in a small equivalent serial $R_{L_{coldStart}}$. A better matching network is suggested in the future work section to convert the load impedance to a better optimized R_L in order to improve the overall PDL.

III. SIMULATION AND MEASUREMENT RESULTS

From Fig. 4, we can conclude that when the R_L is around 18–43 ohm, a 3-coil system (two receiver coils) has a better PDL if k_{12} is around 0–0.45. In comparison, a 2-coil system will have a better PDL if k_{12} is above 0.45 (given similar R_s

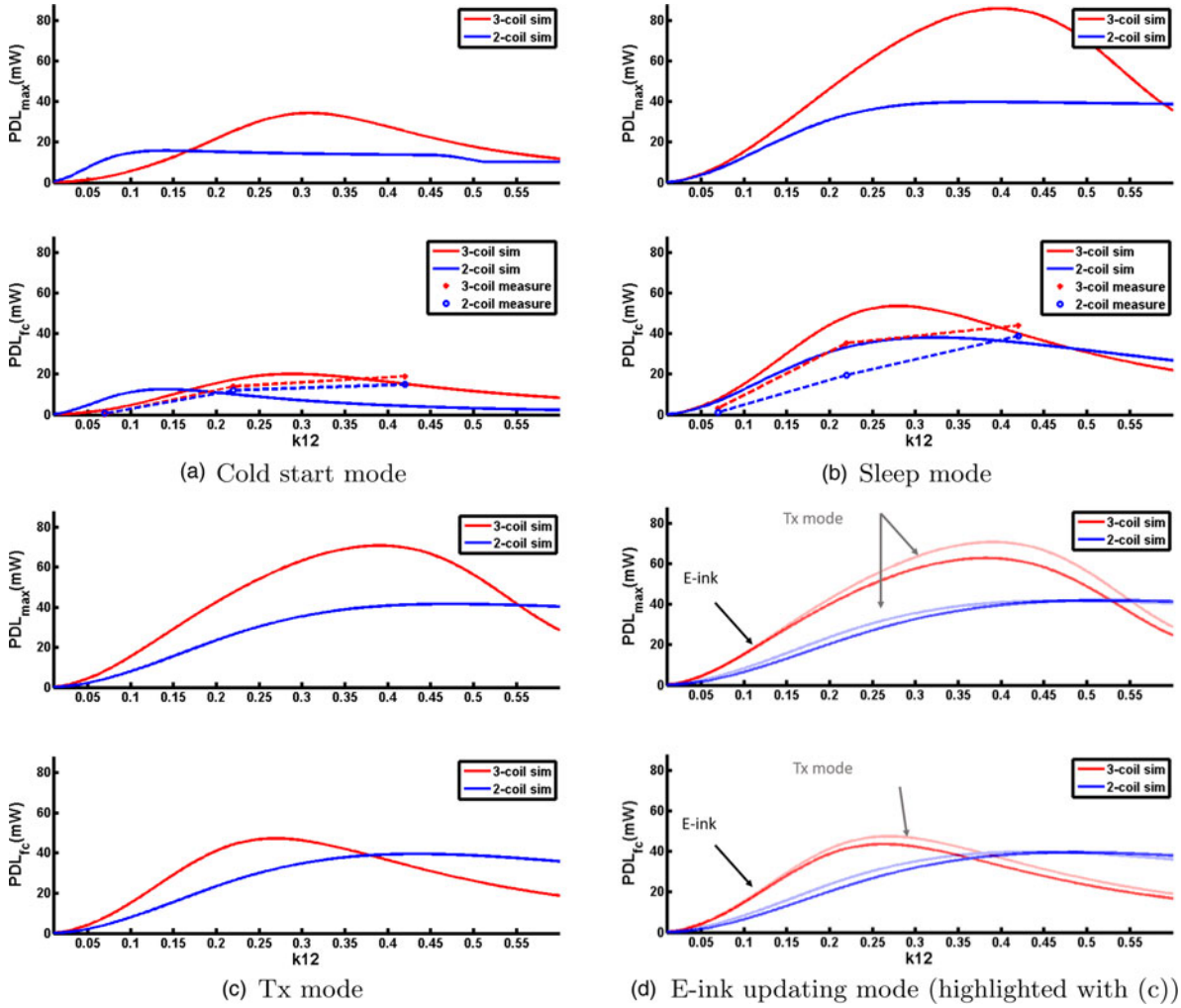

Fig. 4. The simulated and measured PDL of NFC-WISP 2.0 (includes antenna parasitic effects and detuned L_2): PDL_{max} is the maximum PDL at the resonant frequency(which may shift away from 13.56 MHz) when sweeping transmitted frequency. The PDL_{fc} refers to the PDL when only transmitting a 13.56 MHz signal from an NFC reader. The simulated k_{12} is between 0 and 0.6, however, in an NFC-WISP system, k_{12} is around 0–0.42 in practice; the smart-phone case and complex hardware substrate lead to a reduction in the practical maximum for k_{12} to <0.42.

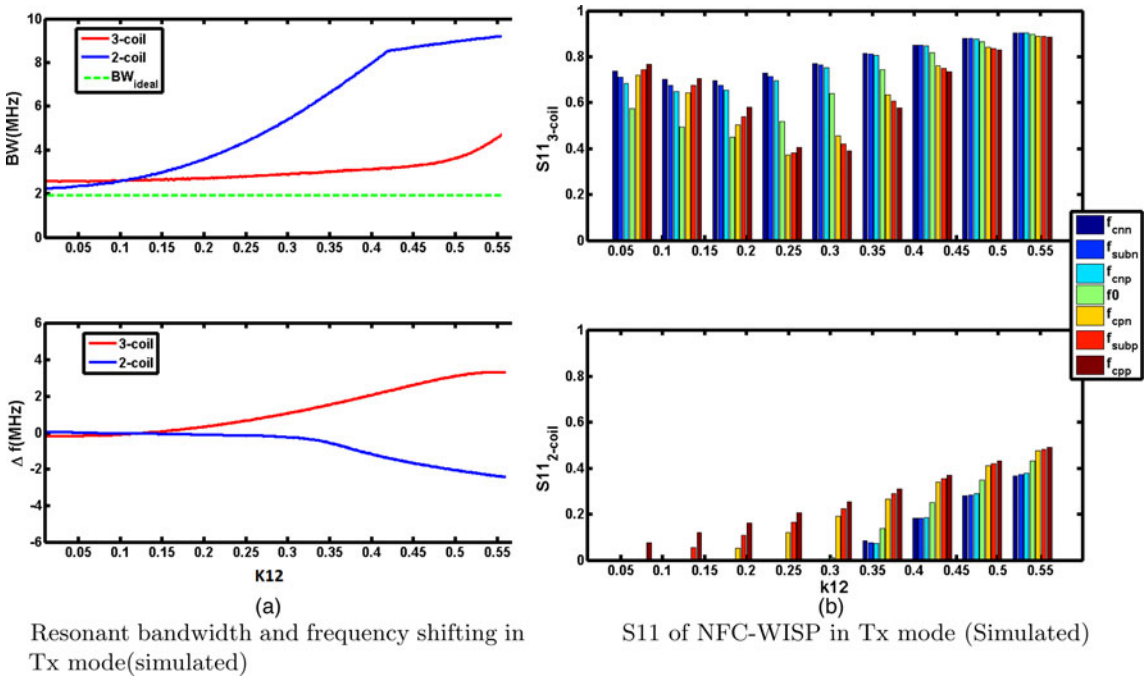

Fig. 5. (a) is the bandwidth performance (includes antenna parasitics and detuned L_2: BW_{ideal} refers to minimum bandwidth required by NFC protocol; the BW refers to the bandwidth of highest PDL (even when two resonant frequency appears) at resonant frequency, the resonant frequency normally shifts away from the NFC frequency as k_{12} increases; Δf is the frequency offset of the highest resonant frequency to 13.56 MHz. In the NFC-WISP system, it is around 0–0.4. (b) is the S11 of NFC load modulation spectrum, $fo = 13.56MHz$, $f_{sub} = 847.5KHz$, $f_{data} = 105.9KHz$, $f_{subn} = fo - f_{sub}$, $f_{subp} = fo + f_{sub}$, $f_{cnn} = f_{subn} - f_{data}$, $f_{cnp} = f_{subn} + f_{data}$, $f_{cpn} = f_{subp} - f_{data}$, $f_{cpp} = f_{subp} + f_{data}$. (k12 refers to the *Tx*-to-First *Rx* coil in all systems).

showed in Table 1). The measured reading range between NFC-WISP and phone (0−3 cm) results in a calculated k_{12} of 0.42–0. This suggests that a 3-coil system is a better option when power performance is of higher priority than communication. But if a certain application requires the higher PDL while the achievable k_{12} is around 0.42–0.65, then a 2-coil low Q system is suggested. Note that the increase of R_L will change the threshold of k_{12} where the PDL of a 3-coil system and a 2-coil system are equal. The simulation model used in Fig. 4 is based on Fig. 3, which neither include the nonlinear behavior of the rectifier and switch nor the interference of the smart-phone substrate. Besides, the noisy cell phone substrate will reduce the maximum k_{12} below simulated 0.42 in practice. Therefore, the measurement result differs a bit from the simulation.

In general, the frequency of the max PDL will shift away from its original tuning frequency with an increase of k_{12}. That is because the parasitic capacitance and the cross-coupling effect become dominant as the range reduces. By detuning a 3-coil system to a lower frequency rather than to 13.56 MHz, we can shift the NFC-WISP working range. In our experiment, if we detune the high Q receiver coil L_2 to 12 MHz, we can shift the NFC-WISP up-link reading range from 2.8–3 cm to 0.8–1.65 cm. Typically, the PDL and communication performance, particularly the up-link, are very position-sensitive in a 3-coil system, mainly because of the larger frequency shift caused by the higher Q. An empirical suggestion is to detune the high Q coil L_2 of the NFC-WISP at 12 MHz given small k_{12} in order to optimize the PDL within the entire range of 0.5–2cm. The achieved PDL here is sufficient for updating a 2.7″ display (more than 16mJ energy consumption). In conclusion, decreasing the tuning frequency of only high Q receiver coil can shift the operation range for power and communication in a 3-coil system. But a high Q_3-coil system, in general, is very sensitive to changes in relative antenna position.

(a) Cold start mode, (b) Sleep mode, (c) *Tx* mode, (d) E-ink updating mode (highlighted with (c)).

Typically, the NFC-WISP communication range is limited by its up-link. During the up-link (from NFC-WISP to Phone), the 3-coil system experiences a larger frequency shift compared to the 2-coil system, because the 2-coil system has lower Q. while Lower system Q reduces PDL, it ensures more robust communication because of its wide bandwidth as well as the smaller frequency shift. S_{11} is a metric to determine the sensitivity of the up-link in an NFC communication system, lower S_{11} value results in a higher SNR (signal to noise ratio) during load modulation. From Figs 5 and 6, we can also see that the 2-coil system normally has better S_{11} even when considering the frequency shifting effect in *Tx* mode. The NFC 14443 Type B protocol requires at least 1.906 MHz up-link bandwidth [17]. In general, larger bandwidth can provide the capability of higher data rate and higher tolerance to the change of relative antenna position, so the 2-coil system suits for this purpose.

Different application requirements may have distinct priorities in regards to power, communication performance, reading range, and tolerance to the change of relative antenna position. The simulation and measurement results discussed in Figs 4 and 6 and Table 2, can help us choose the optimized configuration for each application based on our requirements.

For example, using a conventional NFC card or smartphone case results in a minimum targeting reading distance of d. Then the application may require NFC tag reading and PDL optimization above the distance of d instead of 0 cm

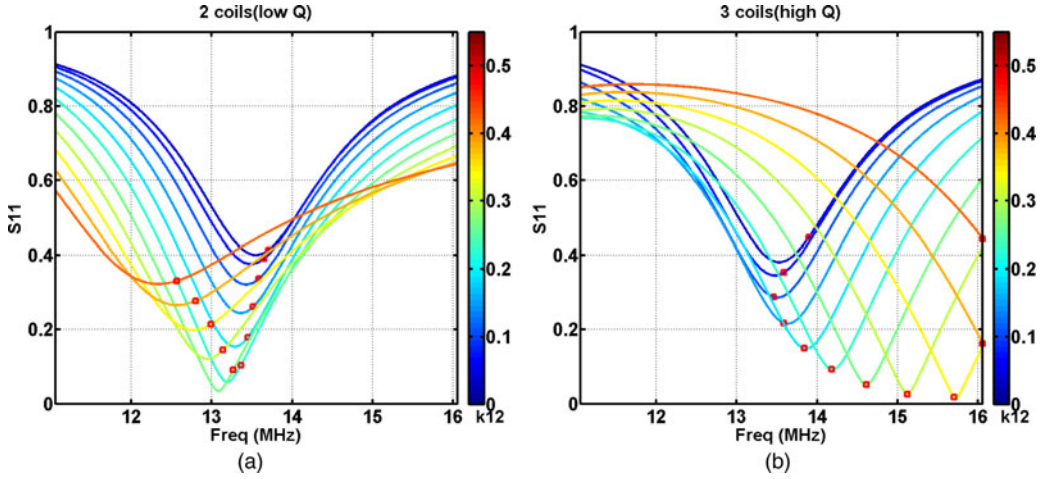

Fig. 6. Simulated S11 of the 2-coil and the 3-coil systems in Tx mode (when $R_L = R_{L_{Tx}}$) by sweeping transmitted frequency (x-axis); red square marks the resonant frequency where the PDL is maximum, the color of each plot refers to the simulation result with different k.

(when the antennas of the reader and the tag have a direct contract with each other). In this scenario, the 3-coil configuration should be chosen without changing the tag antenna design. Another example is that, if moderate and higher PDL and good communication are required over the entire range of 0–3 cm, we can switch to the 2-coil configuration in *Tx* mode and enable a 3-coil configuration in other modes to achieve both higher PDL and better communication. Please note that the optimization threshold of either k_{12}, range or other specs discussed in the paper will vary with different antenna specs in the different systems, but the overall optimization strategy will be similar as what we proposed with NFC-WISP 2.0 and NFC phone reader.

As a result, by implementing this proposed method in the second example, we can use the newly revised NFC-WISP to update a 2.7″ E-ink display within 3s with using a 500 μF capacitor as the charge reservoir and achieve a range of 0–1.5 cm while maintaining a robust communication. The old NFC-WISP hardware had to use a 10 mAh battery to provide sufficient power to update a 2.0″ E-ink display within 0–0.5 cm range and its updating speed is much slower than the NFC-WISP 2.0 hardware. The 2.7″ display consumes around 16 mJ energy, which is two times higher than the required energy for a 2.0″ display in general.

In conclusion, a low Q_2-coil system, which generates low PDL at far range, is less position sensitive and has good communication performance because of lower Q. But, in general, it is very sensitive to changes in load R_L. The high Q_3-coil system can ensure higher PDL and communication at long range and is less sensitive to changes in load R_L. However, it is very sensitive to changes in relative antenna position. Detuning the high Q coil in a 3-coil system can change the optimal reading position where the power performance can be maximized. By switching between low Q_2-coil (in *Tx* mode) and high Q_3-coil configurations (in another mode) in an application, we can obtain the overall optimization of both power and communication performance. The same analysis and approach can be used for other NFC tag optimizations that rely on dynamically adapting the Q value.

Table 2. PDL measurement comparison between the 3-coil and the 2-coil configurations in sleep mode.

Reading range	Estimated k_{12}	Sleep mode (3-coil)	Sleep mode (2-coil)
0.2 cm	0.42	44.16 mW	39 mW
1.25 cm	0.22	35.4 mW	19.57 mW
3 cm	0.07	3.1 mW	1.0 mW

IV APPLICATION

We develop an Android Application (APP) to show one possible usage of the new NFC-WISP 2.0 tag with switchable antenna: a battery-free digital frame (shown in Fig. 7). The APP also has the ability to select an image from any NFC-enabled Android phone, resize and crop the image, process the image to a 1-bit sketch photo, and transfer the image data (which is also transmitting wireless power) to the NFC-WISP tag. The wireless power obtained by the tag from the phone can support updating a 2.7″ or smaller E-ink display by Pervasive Displays [23]. The current APP supports 2.7″ and 2″ displays at the moment.

By clicking the "'IMAGE" button in the application, the user can select any image stored on the phone. After selecting the image, it appears on the application and is ready for manipulation. The user can pinch and drag the image to zoom in/out and resize it to a target frame. After resizing the image to the desired size, the user can click the "'READY" button to keep the frame after cropping and convert it into a 1-bit black-and-white sketch by applying a customized image filter. More image filters, such as Half-toning and Dithering filter, can be implemented in the future to create different image effects. The user can change the size of the image in the application to match the size of the E-ink display on the NFC-WISP tag by clicking toggle button at the top of the application. When the toggle button displays "'large", the current image size corresponds to a 2.7″ E-ink display. When the toggle button displays "'small", the current image size corresponds to a 2.0″ E-ink display. Then, the user can update the battery-free "Display tag" with the resulting sketch by tapping the phone onto the antenna of the tag. The APP can also send notification to

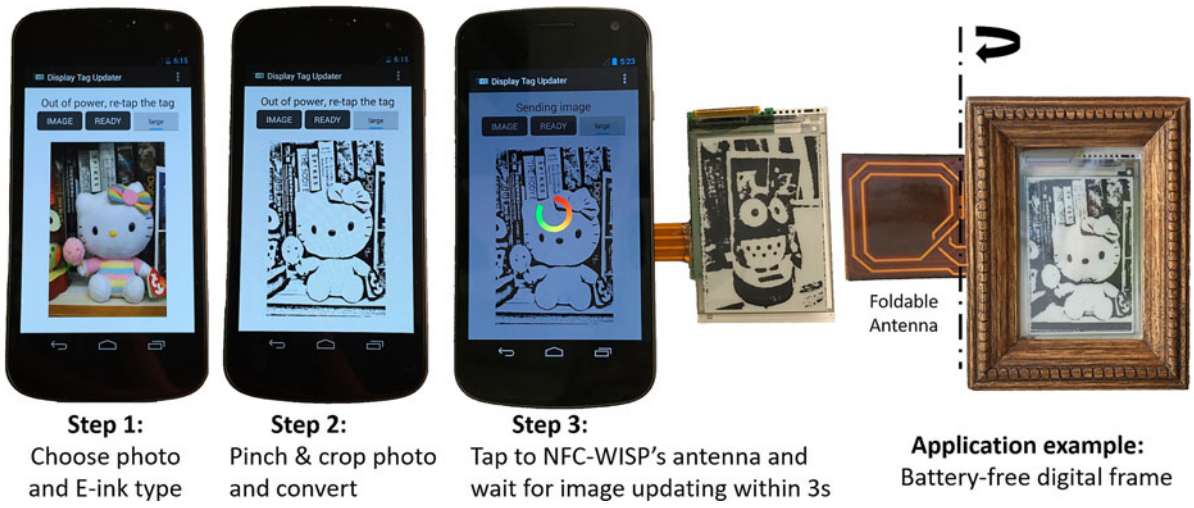

Fig. 7. Updating display NFC-WISP with the designed app.

the user about the state of the NFC-WISP in this application, such as "Tag detected", "Sending image" and "'Out of power, re-tap the tag", to help the user understand the image transfer process and recover the failure by moving the phone away from the tag and re-tap it again. When the phone is in "Sending image state", the screen on the phone will turn dark and a circular progress bar will show the image transfer progress in real-time to remind the user to stay tapped while image transfer is in progress.

The designed NFC-WISP display tag is able to tolerate around 1.5 cm phone-to-antenna position variation and delivers a maximum of 44 mW of power to the NFC-WISP tag with the proper receiver antenna configuration. In this application, the tag switches off the high Q antenna in between the rest of the antennas and turns the system into the 2-coil configuration in Tx mode (to optimize the communication), and switches on the middle antenna and enable the 3-coil configuration in other modes (to optimize the power). In our previous work [1], we could only enable a smaller 2.0″ E-ink display updating (half the size of the 2.7″ one) on the NFC-WISP with the assistance of a thin-film battery at a shorter range ($<$0.5 cm). The battery-free feature of the newly developed NFC-WISP 2.0 display tag results in a lower hardware cost and application barrier. By putting the antenna on the side of the display instead of under the display (compared to the hardware in [1]), the user can observe the change of display and align the cell-phone antenna with the NFC-WISP tag in a better way. Flexible antenna design allows the possibility to mount the tag on a curved surface or fold the antenna under the display when not used.

V. CONCLUSION

This paper presents an adaptive power and communication optimization method based on the simulation and analysis of an NFC wireless power and communication system in both 2-coil and 3-coil configurations. This system consists of a newly developed NFC-WISP hardware with switchable antennas and a commodity NFC-enabled smart-phone. Variations of load R_L and coupling coefficient k between different NFC-WISP operating modes are simulated, and a switchable receiver coil design is proposed and shown to improve both power delivery and communication performance, which can be applied to future NFC wireless power applications. Finally, the use of the proposed method enables a new battery-free NFC-WISP application, in which we can use an NFC-enable smart-phone to update an E-ink display on the passive NFC-WISP tag. Our new design achieves large tolerance to the load variation and antenna alignment. Also, our new design enables operating at a longer distance (improved from 0.5 cm to 1.5 cm) while delivering two times more power than the previous version.

ACKNOWLEDGEMENTS

This work is funded by NSF Award CNS-1305072, Google Faculty Research Award, and Intel Science and Technology Center for Pervasive Computing.

REFERENCES

[1] Zhao, Y.; Smith, J.R.; Sample, A.: Nfc-wisp: A sensing and computationally enhanced near-field rfid platform, in *RFID (RFID), 2015 IEEE Int. Conf. on*. IEEE, 2015, 174–181.

[2] Zhao, Y.; Mahoney, B.; Smith, J.R.: Analysis of a near field communication wireless power system, in *Wireless Power Transfer Conf. (WPTC), 2016 IEEE*. IEEE, 2016, 1–4.

[3] Strommer, E.; Jurvansuu, M.; Tuikka, T.; Ylisaukko-oja, A.; Rapakko, H.; Vesterinen, J.: Nfc-enabled wireless charging, in *Near Field Communication (NFC), 2012 4th Int. Workshop on*. IEEE, 2012, 36–41.

[4] *Ginstr:NFC tags used for health care*. [Online]. Available: http://www.nfc-tracker.com/en/nfc-in-healthcare/.

[5] "*Credit card" heart monitor shares results with NFC*. [Online]. Available: http://www.impakhealth.com/cardiovascular-health.

[6] Coskun, V.; Ozdenizci, B.; Ok, K.: A survey on near field communication (nfc) technology. *Wirel. Pers. Commun.*, **71** (3) (2013), 2259–2294.

[7] Dementyev, A.; et al. "Wirelessly powered bistable display tags," in *Proc. of the 2013 ACM Int. Joint conf. on Pervasive and ubiquitous computing*. ACM, 2013, 383–386.

[8] Zhao, Y.; Smith, J.R.; Sample, A.: "Nfc-wisp: an open source software defined near field rfid sensing platform," in *Proc. of the 2015 ACM International Joint Conference on Pervasive and Ubiquitous Computing and Proc. of the 2015 ACM Int. Symp. on Wearable Computers*. ACM, 2015, 369–372.

[9] *NFC Antenna Design and Application note*. [Online]. Available: http://www.nxp.com/documents/applicationnote/AN11019.pdf.

[10] Wikipedia, "Iso/iec 15693 — wikipedia, the free encyclopedia," 2017, [Online; accessed 23-November-2017]. [Online]. Available: https://en.wikipedia.org/w/index.php?title=ISO/IEC15693&oldid=804776582.

[11] Wikipedia, Iso/iec 14443 — wikipedia, the free encyclopedia, 2017, [Online; accessed 23-November-2017]. [Online]. Available: https://en.wikipedia.org/w/index.php?title=ISO/IEC 14443&oldid=778633053.

[12] Waters, B.H.; Fidelman, P.R.; Raines, J.D.; Smith, J.R.: Simultaneously tuning and powering multiple wirelessly powered devices, in *Wireless Power Transfer Conf. (WPTC), 2015 IEEE*. IEEE, 2015, 1–4.

[13] Kiani, M.; Jow, U.-M.; Ghovanloo, M.: Design and optimization of a 3-coil inductive link for efficient wireless power transmission. *IEEE Trans. Biomedical Circuits Syst.*, **5** (6) (2011), 579–591.

[14] Shin, J.; et al. Design and implementation of shaped magnetic-resonance-based wireless power transfer system for roadway-powered moving electric vehicles. *IEEE Trans. Ind. Electron.*, **61** (3) (2014), 1179–1192.

[15] Hui, S.Y.R.; Zhong, W.; Lee, C.K.: A critical review of recent progress in mid-range wireless power transfer. *IEEE Trans. Power Electron.*, **29** (9) (2014), 4500–4511.

[16] Gubbi, J.; Buyya, R.; Marusic, S.; Palaniswami, M.: Internet of things (iot): A vision, architectural elements, and future directions. *Future Generation Comput. Syst.*, **29** (7) (2013), 1645–1660.

[17] *Wikipedia:ISO/IEC 14443*. [Online]. Available: https://en.wikipedia.org/wiki/ISO/IEC_14443.

[18] Waters, B.H.; Sample, A.P.; Smith, J.R.: Adaptive impedance matching for magnetically coupled resonators, in *Proc. of the PIERS*. Citeseer, 2012, 694–701.

[19] Sample, A.P.; Meyer, D.A.; Smith, J.R. et al.: Analysis, experimental results, and range adaptation of magnetically coupled resonators for wireless power transfer. *IEEE Trans. Ind. Electron.*, **58** (2) (2011), 544–554.

[20] Park, J.; Tak, Y.; Kim, Y.; Kim, Y.; Nam, S.: Investigation of adaptive matching methods for near-field wireless power transfer. *IEEE Trans. Antennas Propag.*, **59** (5) (2011), 1769–1773.

[21] Kurs, A.; Karalis, A.; Mo_att, R.; Joannopoulos, J.D.; Fisher, P.; Soljačić, M.: Wireless power transfer via strongly coupled magnetic resonances. *Science*, **317** (5834) (2007), 83–86.

[22] Cannon, B.L.; Hoburg, J.F.; Stancil, D.D.; Goldstein, S.C.: Magnetic resonant coupling as a potential means for wireless power transfer to multiple small receivers. *IEEE Trans. Power Electron.*, **24** (7) (2009), 1819–1825.

[23] *Pervasive Displays: E-ink Displays*. [Online]. Available: http://www.pervasivedisplays.com/products.

Yi Zhao received her Ph.D. degree in Electrical Engineering from University of Washington, Seattle in 2016.

Huaye Li received a B.S. in Computer Engineering and Electrical Engineering from University of Washington, Seattle in 2017.

Saman Naderiparizi A fifth-year Ph.D. student in the University of Washington Department of Electrical Engineering in Seattle, WA.

Aaron Parks received his Ph.D. degree in Electrical Engineering from University of Washington in 2017.

Joshua R. Smith received his Ph.D. in 1999 from Massachusetts Institute of Technology. Currently, he is an Associate Professor of Computer Science and Engineering, Electrical Engineering department of University of Washington, Seattle.